Article

The Performance of Filava-Polysiloxane, Silres® H62C Composite in High Temperature Application

Klaudio Bari * [ID] **and Thozhuvur Govindaraman Loganathan**

School of Engineering, Telford Innovation Campus, University of Wolverhampton, Telford TF2 9NN, UK;
l.thozhuvurgovindaraman@wlv.ac.uk
* Correspondence: K.Bari@wlv.ac.uk; Tel.: +44-1902-32-3845

Abstract: The research aim is to investigate the performance of novel enriched mineral fibres (Filava) in polysiloxane SLIRES H62 resin. Specimens were manufactured using a vacuum bagging process and oven cured at 250 °C. Specimens were prepared for flexural testing according to BS EN ISO 14125:1998 to obtain flexural strength, modulus, and elongation. The mechanical strength was compared to similar composites, with the aim of determining composite performance index. The flexural modulus (9.7 GPa), flexural strength (83 MPa), and flexural strain (2.9%) were obtained from a three-point bending test. In addition, the study investigates the thermal properties of the composite using a state-of-art Zwick Roell high temperature tensile rig. The results showed Filava/Polysiloxane Composites had an ultimate tensile strength 400 MPa, Young's modulus 16 GPa and strain 2.5% at 1000 °C, and no smoke and ash were observed during pyrolysis. Ongoing research is currently taking place to use Filava-H62 in fire-retardant enclosure for lithium-ferro-phosphate Batteries used in electric trucks.

Keywords: Filava fibre; polysiloxane resin; fire retardant composite; LIB enclosures; lithium ferro phosphate battery; high temperature tensile testing

1. Introduction

The demand for lithium-ion battery (LIB)-powered road vehicles continues to increase around the world. As more of these become operational across the globe, their involvement in traffic accidents and fire incidents is likely to rise. This can damage LIB and subsequently pose a threat to occupants and responders as well as those involved in post-crash operations [1].

Automakers are building electric cars with increasing driving ranges and charging cycles. However, the large batteries and the high energy density become more challenging due to their fire and explosion hazard, making important the need to develop reliable housing that safeguards from these hazards. Many new enclosure concepts have been developed to meet these challenges; however, they are not either ready for series production due lack of economic feasibility or cannot withstand an excess temperature of 500 °C [2].

Very large batteries, usually mounted in the vehicle's underbody, typically consists of several small cells in a sealed enclosure made of aluminium alloy, CFRP, basalt epoxy composite, or steel. Every battery housing has a cover, so the entire battery need not be discarded if small defects appear. Accessibility to the battery unit is important for repairs and at the same time road sprays are not permitted to intrude through the gap between the cover and the housing. In addition, thermal management system and venting system become more complicated and expensive; hence, the demand has been raised for more simple enclosure that can act passively during thermal runaway or external damage to the cells [3]. Figure 1a,b shows our CAD concept for LIB battery power pack for electric car, highlighting the battery management system (BMS), battery cooling system (BCS), and the output power.
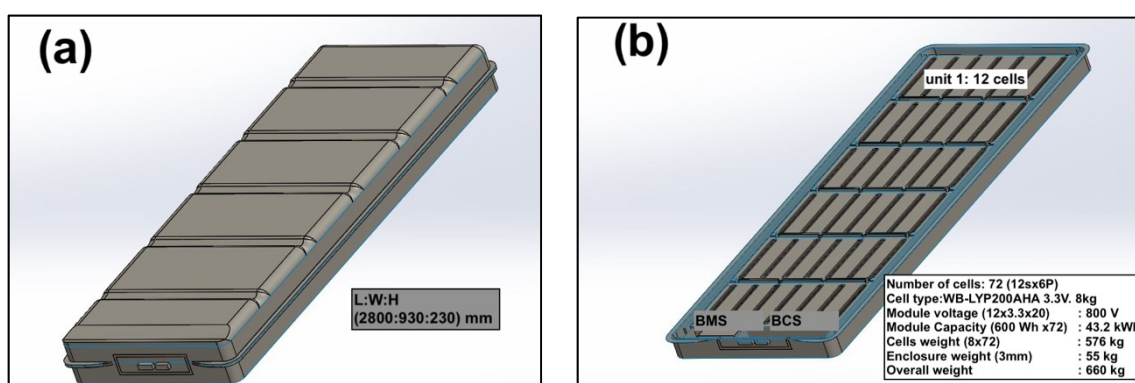
Figure 1. CAD concept of electric car power module (**a**) scalability of the module, (**b**) Electric detail of the internal parts in the power module.

The excellent thermal performance of Filava fibre stated by manufacturers exhibited good mechanical properties up to 950 °C. By contrast, carbon fibre epoxy composite had turned to ash at 500 °C. This has made Filava fibres an excellent suitable material for automotive exhaust and braking pads [4], as the fibres are nearly incombustible and emit low smoke and ash when exposed to a high temperature flame as shown in the video [Supplementary Video S1]. The fire-resistant properties make Filava fabrics highly suitable for fire retardant application for interior components in road vehicles and aircraft [5]. Additional industrial applications of Filava fibres include the marine application, where fibres can be used to reinforce Hulls in high performance yachts [4]. In order to make the fibre compatible with any resin, sizing of fibres were done by various chemical etching processes using certain abrasives to suit the wettability of resin. Filava fibres are currently used in the manufacture of hybrid composites with other fibres such as carbon fibres, where multiple intra-plies are combined in a common matrix to elevate desirable properties [4].

It is well understood that Filava fibre is one of the prominent fibre candidates in the composite industry to compare with Supplementary Video S2 glass fibres. Currently, a research study is taking place to enhance the mechanical and thermal properties of the reinforcement fibre to specifically support high-temperature and lightweight applications [6]. Filava as a volcanic rock fibre is aggregated and enriched with various mineral additives with the aim to increase and guarantee isotropic mechanical and chemical properties. A precisely defined confidential ingredient of mineral composition is added to volcanic rock and blended in the melt pool of the fusion induction furnace to draw the optimized fibres [4].

The Filava fabric, shown in Figure 2a, has been manufactured by Isomatex/Belgium, with an improvement in property from ordinary basalt through the addition of a proprietary blend of minerals and a tailor-made sizing process. Filava fibre was selected in this work due to its unique thermal properties compared with basalt fibre and their increasing popularity in the automotive sector. A highly flexible Filava/Polysiloxane Composite (FPC), shown in Figure 2b, had a high versatility in shape and geometry unlike Nextel 3M alumina fibres composite [7].
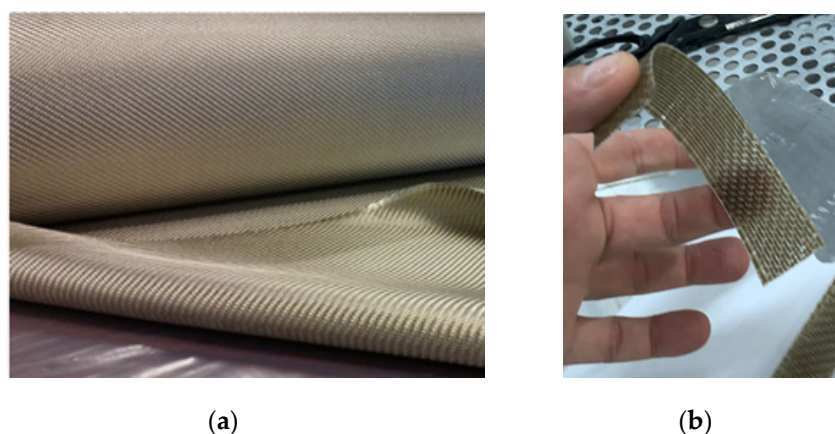
(**a**)　　　　　　　　　　　　　(**b**)

Figure 2. (**a**) Twill 2 × 2, 3K Filava fabric; (**b**) Flexible FPC specimen of 0.5 mm thickness.

Table 1 explicitly shows the mechanical properties of E- glass, carbon, ordinary basalt, and Filava fibres, tested based on standard ISO 3341. The yarn used for the tests were sized and dried roving, which consist of thousands of continuous elementary filaments bonded into a single strand. The major advantage of Filava is their high service temperature and excellent mechanical properties. Further, on considering the energy consumption to produce fibres, Filava consumes 8.5 kWh/kg and stands ahead of glass fibre, which takes 9.3 kWh/kg [8].

Table 1. The tensile properties of E- glass, carbon, ordinary basalt and Filava fibres as per ISO 3341 [8].

Fibre	Tensile Properties			Service Temperature (°C)	Density (g/cm^3)
	Strength MPa	Modulus GPa	Strain %		
E-glass	<1100	74	1.9	480	2.6
Carbon	1850	250	<0.9	<550	1.76
Basalt	1580	80–90	2.0	<550	2.73
Filava	1950	90–100	2.3	720	2.61

Regarding its thermal properties, Filava has been reported to have a melting point of 1560 °C and a glass transition temperature (Tg) of 950 °C [4]. In general, Filava products have an application temperature range of −200 to +850 °C with very high corrosion resistance and alkali-resistance. Woven fabrics made of Filava are almost incombustible and, in case of fire, produce no smoke and toxic fumes as shown in the video [Supplementary Video S1]. It is interesting to know that Filava shows no sign of shrinkage even at 740 °C [4]. This combustion behaviour provides an added value to the safe escape of occupants before dense and toxic smoke being accumulated. Filava fibres are quite suitable for a lot of industrial applications amongst automotive, aerospace, ballistic, wind turbine, and sport goods. Also, it exhibits good wettability because of tailorable sizing to accommodate different resin chemistries. To meet the industrial requirements, the woven fabrics made of Filava were manufactured with three different fabric patterns: plain, twill, and satin, as shown in Figure 3.
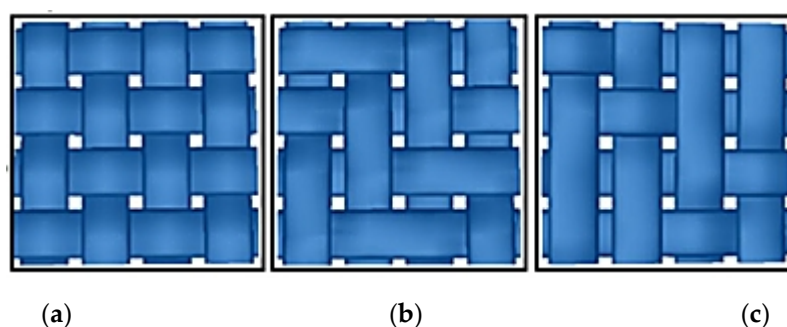
Figure 3. Schematic representation of weave pattern: (**a**) Plain; (**b**) Twill; (**c**) Satin.

To address the need for fire retardant enclosure for Lithium-Ion batteries (LIB) used in road vehicles, this work's aim is to partially investigate the mechanical and thermal properties of FPC to validate their application in electric vehicles.

The current main battery enclosure for electric vehicles is made from aluminium alloy or CFRP that integrate the battery and thermal management system (BMS, TMS). Battery tractions must be significant in size in order to achieve sufficient driving ranges and supply the required voltage and current to the induction motors. Such types of battery pack systems take up a lot more space than fuel tanks due their low energy density compared to gasoline or diesel. Specifically, 0.1–0.2 kWh/kg versus more than 10 kWh/kg for conventional fuels [2]. This also means that the traction battery contributes to a large portion of the vehicles total weight. For example, the battery pack in the electric Scania L 320 6 × 2 truck makes up 30% of its total weight (20 tons) [1]. There are two options to deploy them in trucks: by placing relatively heavy packs on top of a vehicle, which makes it more difficult to obtain a low center of gravity. In addition, roof mounted solutions require protection from debris and moisture accumulation. Alternatively, by placing them at bottom of a vehicle, which generates more risk for collision and damage in the event of a severe road accident. In such a scenario, the flame from a LIB can result in severe consequences, in terms of human injury or death. It is well known that molten aluminium is very reactive with water or with cathode electrolyte in case of sudden fire in electric vehicles, these flammable materials will act against the fire suppresser and spread the fire to a wider range [9].

A comparison of different basalt and Filava fibres properties are listed in Table 2. It is evident from the comparison that the properties of basalt fibre vary significantly based on manufacturer and location [10], which is due to the varying geological mineral basalt rock and location and depth of the mine. It is widely understood that ingredients within the basalt rocks can influence their properties. For example, an increased aluminium oxide content in the basalt improves the mechanical properties whilst an increase of iron oxides decreases its mechanical properties [11].

Table 2. Comparison of Filava fibres to various basalt fibre according to ASTM D2343.

Manufacturer and Country of Origin	Isomatex, Belgium	Basaltex, Belgium	Mafic, USA Basalt	China Basalt
Elastic Modulus, GPa	86–97	85–89	86–92	78–84
Tensile Strength, MPa	3400–3800	2900–3100	2900–3100	2583–2793
Elongation at Break, %	4	-	3.5	3.4–3.9
Density, g/cm^3	2.6	2.67	2.63	-
Standard Operating Temperature, °C	720	600	-	-
Cost, €/kg	€€€	€€	€	€
References	[8]	[12]	[12]	[13]

2. Materials and Specimen Preparation

Filava-Polysiloxane Composite (FPC) was manufactured using the vacuum bagging process. Filava dry fabric 3K, 2 × 2 twill pattern (Figure 2b) with areal density 200GSM was used as reinforcement fibres. A commercially available methylphenylvinylhydrogen polysiloxane, Silres® H62C produced by Wacker Chemie AG (Burghausen, Germany) was used as a resin [14]. The shrinkage of the resin was modified using 1 wt.% silica nano particles filler.

The aluminium mould plate was polished to 20-micron finish and coated with a thin layer of release agents. On the prepared aluminium plate, 5 plies of Filava fabric were hand laminated with 60 vol% of polysiloxane resin. The Vacuum bag, peel ply and breather fabric that were used in the manufacturing process were purchased from Easy Composites Ltd as shown in Figure 4a. Specimens were cut in the dry fabric state to the bespoke size in order to avoid crack formation in the event of slicing a sheet into specimens after curing (Figure 4b). Previous research shows that cutting specimens after curing is detrimental and has an impact on the validity of the results due to the appearance of de-laminations and crack formation [15]. The cured specimen is shown in Figure 4c.
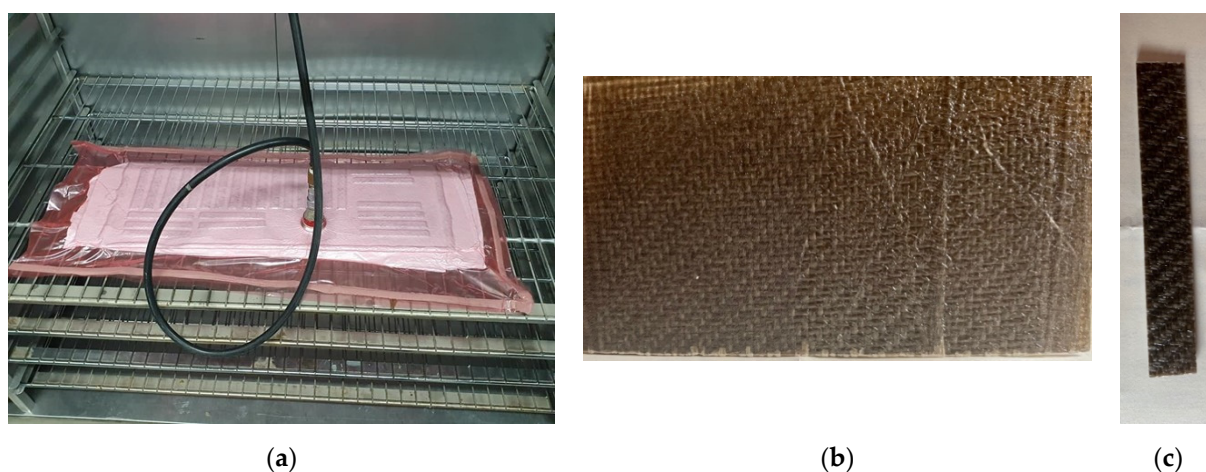

| (a) | (b) | (c) |

Figure 4. (**a**) Preparation of vacuum bagging; (**b**) Surface texture of the specimen; (**c**) Specimens after curing.

The curing cycle consists of two parts; initial gelling phase for 2 h to reduce resin viscosity and improve resin wettability, followed by second stage heating at 250 °C for 2 h. In accordance with manufacturer recommendations, the curing cycle was designed to ensure complete polymerization of the matrix. After curing, the specimens were taken out of the oven and fine trimmed using an abrasive cutting wheel cooled by a water. The specimen was found to have density 1.45 g/cm^3, coefficient of thermal expansion 3.02×10^{-6} °C^{-1} and thermal conductivity 1.09 w/m.k.

3. Experimental Section

3.1. Three-Point Bend Test

The flexural properties were obtained by doing three-point bend test in accordance with BS EN ISO 14125:1998 class IV (Figure 5a) utilizing a Zwick Roell 1474 universal testing machine as shown in Figure 5b. Specimen dimensions are provided in Table 3. The displacement rate in the test was set at 5mm/min and specimen deflection was measured by built-in extensometer. Equations (1)–(3) were used for the calculation of flexural modulus, stress and elongation [15].

$$\text{FlexuralStress} \quad : \quad \sigma_f = \frac{3FL}{2bh^2} \tag{1}$$

$$\text{FlexuralModulus} \quad : \quad E_f = \frac{L^3}{4bh^3}\left(\frac{\Delta F}{\Delta S}\right) \tag{2}$$

$$\text{Strain} \quad : \quad \in = \frac{6Sh}{L^2} \tag{3}$$

where: F-Load (N), L-support Span (mm), h-thickness (mm), b-width (mm), and S-displacement (mm)
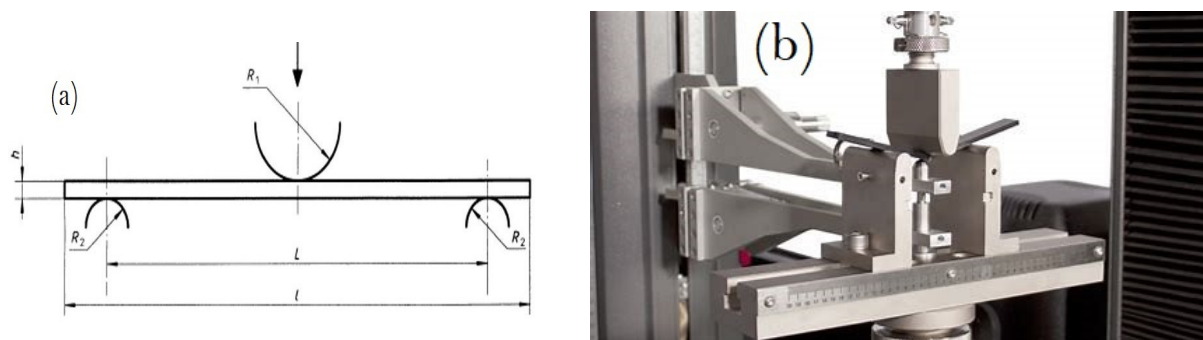

Figure 5. Flexural test set up (**a**) sketch of 3-point bend, where R1, R2, and h: 10, 5, and 2.15 mm, respectively, (**b**) Zwick Roell universal testing machine.

Table 3. Test specimen dimensions.

Specimen	Length, mm	Support Span (L), mm	Width (b), mm	Thickness (h), mm
1	100	80	15.78	2.15
2	100	80	15.01	2.14

3.2. Fractography

Zeiss Sigma VP Field Emission Scanning Electron Microscopes (SEM) available at the University of Wolverhampton were used to examine the failure mode at interface fibre/matrix. The basic approach entails developing an understanding of the fundamental failure modes and mechanisms associated with the sizing process that took place at the fibre manufacture site. This knowledge can then be implemented for tailoring advanced abrasive ingredients [16].

3.3. Thermal Tensile Testing

The aim of the test was to examine the strength of FPC in the event of LIB sudden fire bust inside their enclosures. Although there is a safety venting valve built-in in any enclosure, it is common that these valves become faulty with passing time due to spring failure, or they were blocked by internal debris from the cooling management system inside the enclosure [17]. In the event of extreme LIB thermal runaway, some of the inevitable incidents such as short circuit, punch damage, or voltage overcharge and discharge, a simultaneous raise of pressure and temperature inside cells could occur. This is a very common phenomena in Lithium Ferro Phosphate (LFP) batteries, which are used mainly in electric cars due to their stable voltage supply during operation [9]. Hence, the thermal strain test was tailored to demonstrate this scenario by using a high temperature tensile testing rig (Zwick Roell in Germany) shown in Figure 6. This arrangement ascertains both tensile force and temperatures to be applied simultaneously according to standard ISO 6892-2 till failure. Specimen with dimension (L × W × h) (100, 15, 2 mm) is gripped between two ceramics jaws and exposed simultaneously to an increasing temperature from 20 to 1000 °C ramped at rate 10 °C/min and a tensile force rate 100 N/min in argon environment. The test was conducted on five samples and each test lasts 120 min.

A ceramic built in extensometer was attached to the specimen to detect one-directional displacement. TestXpert/research software was used to record the data and exported in a digital format [18]. Thermal strain plots exported into excel format to understand the correlations between force-displacement-temperature.
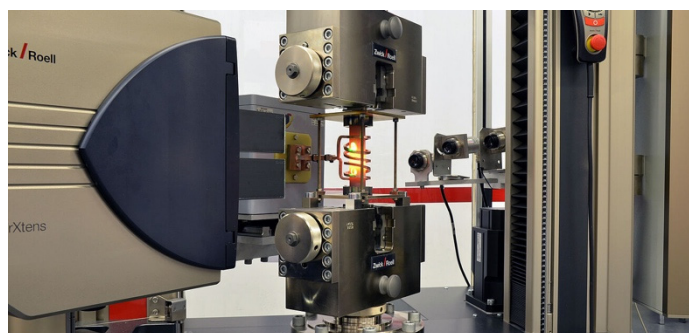

Figure 6. Zwick Roell thermal strain testing rig.

4. Results

Flexural force-deflection plots of the FPC specimens 1 and 2 obtained during the three-point flexural test is shown in the Figure 7. A linear gradient of the elastic region indicates the balanced fibre orientation in the X,Y directions in twill weave pattern. Table 4 shows the maximum flexural strength, modulus, and strain, calculated using Equations (1)–(3).
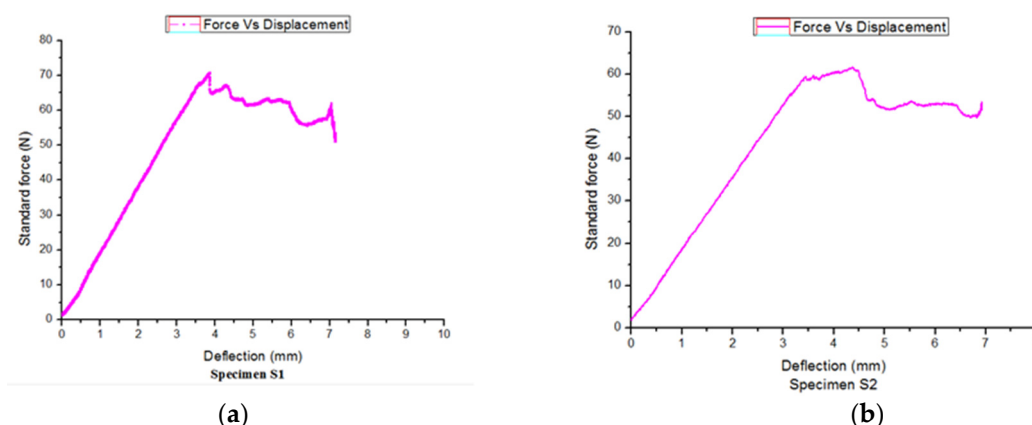

(**a**)

(**b**)

Figure 7. Flexural testing plots of test specimens: (**a**) Sample 1, (**b**) Sample 2.

Table 4. Flexural modulus, flexural strength, and Elongation.

Specimen	Max. Load (N)	Displacement at Failure (mm)	Stiffness (N/mm)	Flexural Modulus (GPa)	Flexural Strength (MPa)	Maximum Flexural Strain, %
Sample 1	71	3.8	18	9.463	83.27	2.89
Sample 2	62	4	16.5	9.779	80.01	2.87

The initial observation from the flexural testing indicates the mechanical performance of the FPC is lower than normally anticipated due to low curing temperature (250 °C) and the aspect ratio L:h was 40:1 and used in the mechanical testing standard. We think that the three-point flexural test is an optimum testing method of LIB enclosure that stimulated point heavy load cells in the middle section of the enclosure.

From the fractography examination of failing flexural specimens, we have examined the surface texture of the pull-off fibres. The sizing of Filava fibres has successfully created

surface ridges that clearly indicate an enhancement in the fibre/matrix interface, which contributes to the enhancement of Interlaminar Shear Strength ILSS, as shown in Figure 8a. There are no sign of delamination or cohesive cracks observed in the cross-sectional view of the failing specimen as shown in Figure 8b.
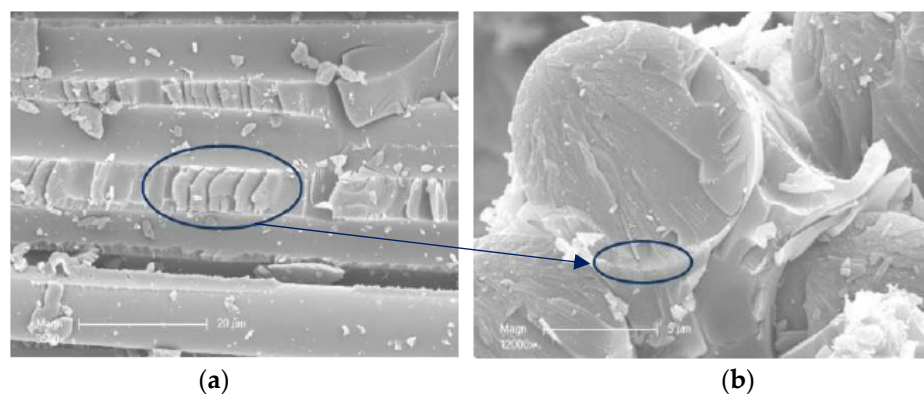

(**a**)   (**b**)

Figure 8. SEM images shows the effect of fibre sizing (**a**) surface ridges and (**b**) fibre matrix interface.

From the thermal tensile test and force/deformation, a plot was obtained during the specimen thermal cycle from room temperature to 1000 °C, as shown in Figure 9a. There is a clear non-linear correlation between tension force and deformation till failure at 2.5% strain at 1000 °C. The deformation and tensile force curve at elevated temperature is shown in Figure 9b. The ultimate tensile strength was calculated as (12,000 N/30 mm^2 = 400 MPa) and tension modulus was calculated as (400 MPa/0.025 = 16 GPa).
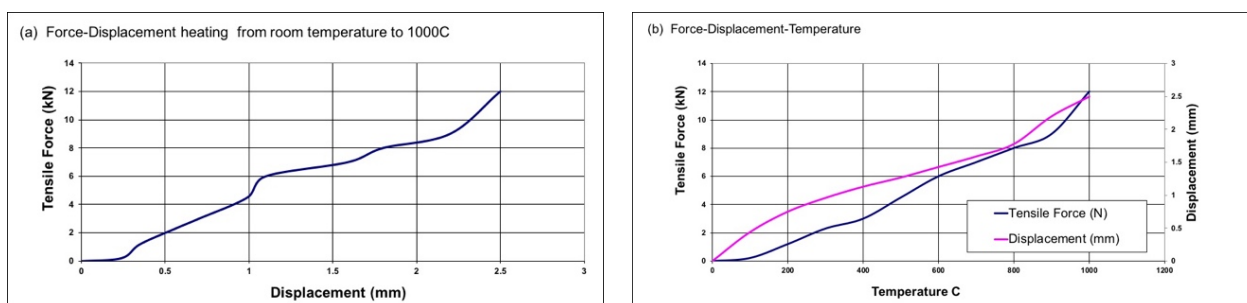

Figure 9. Thermal strain curve of FPC shows (**a**) Force displacement, (**b**) temperature, Tensile force and strain correlations.

5. Discussion

Basalt fibres can produce low cost and environmentally friendly composites with moderate mechanical and thermal properties and are becoming increasingly popular within the automotive sector. However, Filava fibres have enhanced mechanical and thermal properties which exceed conventional basalt fibres through the additional minerals in their chemistry and customer-made sizing that suit specific matrix chemistry. Nonetheless, the density of FPC (1.45 g/cm^3) is lower than the equivalent carbon, aramid or glass fibres epoxy composite. It was reported in a previous research that flame temperature of LIB can reach up to 900 °C in the worst case scenario [5]. High softening temperature (950 °C) and acceptable service temperature (720 °C) of FPC makes it suitable as a fire-retardant composite in LIB enclosures. In particular, no smokes or ash generation shown in the video [Supplementary Video S2] fit the aerospace requirement, where airplane's air-condition supplies limited amount of oxygen in case of onboard fire.

The various performance indices of competitor composite materials are listed Table 5 according to their fibre volume fraction, orientation, stacking sequence and matrix type. FPC flexural properties were compared to epoxy resin base composite relevant to the

application. Although, it is difficult to find identical volume fibre fractions in the literature, the data in Table 5 provides an overview of the various composite flexural properties. As expected, carbon fibre epoxy composite shows higher flexural strength than FPC, hence, our future research will focus on developing intra-plies weave patterns using carbon fibre to form a hybrid composite. Samples have been already sent to Carr reinforcement company in UK to produce state-of-art 3×3 twill Intra-plies fabric that allocated for LIB enclosure in electric trucks.

Table 5. Flexural strength of FPC with an equivalent Basalt, carbon, E-glass epoxy composite flexural according to BS ISO 14125.

Manufacture Source	Present Findings	Bari et al. (2020) [15]	Gadow et al. (2019) [12]	Lopresto et al. (2011) [13]	Lopresto et al. (2011) [13]
Fibre Manufacturer and Country of Origin	Isomatex, Belgium Filava	Solvay, UK Carbon	Kamenny Vek, Russia Basalt	ZLBM, Germany Basalt	E-glass
Fibre orientation	2×2 twill	2×2 twill	Plain weave	Plain weave	Plain weave
V_f %/gsm	40/200	50/200	60/210	51/200	50/200
Matrix Type	Polysiloxane H62	Epoxy	Polysiloxane H62	Epoxy	Epoxy
Flexural Modulus, GPa	9.46–9.78	30	19–36	23	25
Max. Flexural Strength, MPa	83	195	Not reported	50	75
Density g/cm^3	1.45	1.75	Not reported	1.86	1.85

The thermal and mechanical stability of FPC is an interesting feature in using in applications where high temperature, lightweight, and impact resistance are needed. Gadow et al. [12] demonstrated a successful application of high temperature properties in basalt polysiloxane H62 composite; however, the mechanical properties were significantly decreased at elevated temperature. In addition, lower density of FPC compared with CFRP, BFRP, and GFRP will reduce the weight of the EV and hence increase the overall energy density of the battery pack module.

Non-linear thermal strain-stress behaviour was observed in Figure 9a,b during the increase of temperature and the strain values seemed to fluctuate during the test. This might be related to the common occurrences on ceramic shrinkage at elevated temperatures [10]. The shrinkage force acts opposite to the direction of tensile force, hence affecting the strain values. This will bring some uncertainty to the obtained values of stress, strain, and Young's modulus. However, the main idea from the test is to predict the mechanical strength of FPC at 1000 °C, so the design criteria for the enclosure can be established and accurate thickness can be concluded in designing a bespoke enclosure. There are other vital tests that need to be conducted before commercialization, such as drop weight, humidity, vibration, and water immersion examination.

Isomatex is working on a project to improve to the surface texture of the fibre by surface coating with alumina particles to increase thermal stability in excess of 1100–1250 °C. The modified fibre are considered to be a genuine alternative to 3 M Nextel fabrics, which are rated at service temperature 1200–1300 °C and are ten times more expensive than Filava fibres [7]. The cost of enclosures will play a vital role in decreasing the cost of electric car production in the future.

It is important to note that the UK government are intending to introduce a new legislation to enhance the fire safety regulation of LIB in electric vehicles that will end the IC vehicle legacy by 2035.

6. Conclusions

Filava-polysiloxane is a novel composite (FPC) developed in-house in collaboration with Isomatex. It is a cost-effective material that is affordable for middle class SMEs and the work is aimed to regain public trust in LIB, which are susceptible to fire hazards. The composite category (FPC) is positioned between inexpensive glass fibre (such as E or S glass fibre) and expensive ceramic fibres (such as Alumina or SiC fibres). The flammability temperature of LIB is proven to be below the softening temperature of FPC. The examination for the FPC performance presented the following observations:

1. The physical properties such as elongation at break (2.5%), density (1.45 g/cm^3) and thermal properties such as softening temperature (950 °C) and service temperature 720 °C offer attractive opportunity in using FPC as enclosures for electric road vehicles, in particular heavy vehicles in excess of 3.5 ton (buses or trucks).
2. The high temperature tensile test indicates promising mechanical properties at 1000 °C, such as UTS (400 MPa), Young's modulus (16 GPa) and elongation (2.5%), which presents the birth of a new competitor to aluminium and CFRP that are currently used in LIB enclosure.
3. The flexural properties of FPC indicates a necessity to strengthen its weave structure by either introducing intra-plies of carbon/Filava fibres and/or designing a sandwich panel with core/skin configuration.
4. A successful sizing process of Filava fibre to silicon-based resin shows high tenacity interface through the formation of ridges at the interfaces. This will enhance both Interlaminar Shear Strength (ILSS) and in-plane shear strength.
5. A future work will be focused on in-situ examination of FPC enclosure in the event of fire scenario at air environment using certified fire testing rigs. This has been planned to be conducted at the Fraunhofer Institute of High Temperature Ceramics Bayreuth in Germany.

References

1. Ge, S.; Leng, Y.; Liu, T.; Longchamps, R.S.; Yang, X.-G.; Gao, Y.; Wang, D.; Wang, D.; Wang, C.-Y. A new approach to both high safety and high performance of lithium-ion batteries. *Sci. Adv.* **2020**, *6*, eaay7633. [CrossRef] [PubMed]
2. Bisschop, R.; Willstrand, O.; Rosengren, M. Handling Lithium-Ion Batteries in Electric Vehicles: Preventing and Recovering from Hazardous Events. *Fire Technol.* **2020**, *56*, 2671–2694. [CrossRef]
3. Chen, T.; Jin, Y.; Lv, H.; Yang, A.; Liu, M.; Chen, B.; Xie, Y.; Chen, Q. Applications of Lithium-Ion Batteries in Grid-Scale Energy Storage Systems. *Trans. Tianjin Univ.* **2020**, *26*, 208–217. [CrossRef]
4. Isomatex, S.A. Advanced Fibre Manufacturer. Available online: https://www.nae.fr/wp-content/uploads/2019/01/Presentation-ISOMATEX_20181218.pdf (accessed on 12 February 2021).
5. Ghiji, M.; Novozhilov, V.; Moinuddin, K.; Joseph, P.; Burch, I.; Suendermann, B.; Gamble, G. A Review of Lithium-Ion Battery Fire Suppression. *Energies* **2020**, *13*, 5117. [CrossRef]
6. Short, G.; Guild, F.; Pavier, M. Delaminations in flat and curved composite laminates subjected to compressive load. *Compos. Struct.* **2002**, *58*, 249–258. [CrossRef]

7.   Pritzkow, W.E.; Almeida, R.S.; Mateus, L.B.; Tushtev, K.; Rezwan, K. All-oxide ceramic matrix composites (OCMC) based on low cost 3M Nextel™ 610 fabrics. *J. Eur. Ceram. Soc.* **2021**, *41*, 3177–3187. [CrossRef]
8.   Voss, B. Filava Fibre Material Data Sheet. 2019. Available online: www.isomatex.com (accessed on 12 February 2021).
9.   Kong, L.; Li, C.; Jiang, J.; Pecht, M.G. Li-Ion Battery Fire Hazards and Safety Strategies. *Energies* **2018**, *11*, 2191. [CrossRef]
10. Mills-Brown, J.; Potter, K.; Foster, S.; Batho, T. The development of a high temperature tensile testing rig for composite laminates. *Compos. Part A App. Sci. Manu.* **2013**, *52*, 99–105. [CrossRef]
11. Landucci, G.; Rossi, F.; Nicolella, C.; Zanelli, S. Design and testing of innovative materials for passive fire protection. *Fire Saf. J.* **2009**, *44*, 1103–1109. [CrossRef]
12. Gadow, R.; Weichand, P.; Jiménez, M. Process Technology, Applications and Thermal Resistivity of Basalt Fiber Reinforced SiOC Composites. *Ceramics* **2019**, *2*, 298–307. [CrossRef]
13. Lopresto, V.; Leone, C.; De Iorio, I. Mechanical characterisation of basalt fibre reinforced plastic. *Compos. Part B Eng.* **2011**, *42*, 717–723. [CrossRef]
14. Wacker SILRES H62C Datasheet. Available online: https://www.wacker.com/h/en-us/medias/SILRES-H62-C-en-2021.01.15.pdf (accessed on 12 February 2021).
15. Bari, K.; Sen, S.; Gulia, K. Experimental and simulation study of the effect of cut-out defect in carbon fibres twill weave composite. *SN Appl. Sci.* **2020**, *2*, 1–13. [CrossRef]
16. Bari, K.; Rolfe, A.; Christofi, A.; Mazzuca, C.; Sudhakar, K. Forensic investigation of a failed connecting rod from a motorcycle engine. *Case Stud. Eng. Fail. Anal.* **2017**, *9*, 9–16. [CrossRef]
17. Bari, K.; Khan, S.Z.; Lowe, T.; Farooqi, J.K. Measurement of thermal diffusivity for alumina borosilicate glass bearing TRISO fuel particles: Experiment and modelling correlation. *J. Mater. Sci.* **2013**, *48*, 4866–4875. [CrossRef]
18. Bari, K.; Osarinmwian, C.; López-Honorato, E.; Abram, T.J. Characterization of the porosity in TRISO coated fuel particles and its effect on the relative thermal diffusivity. *Nucl. Eng. Des.* **2013**, *265*, 668–674. [CrossRef]